Anisotropic pressure molecular dynamics for atomic fluid systems

2007 J. Phys. A: Math. Theor. 40 8585

(http://iopscience.iop.org/1751-8121/40/29/026)

IOP Publishing Journal of Physics A: Mathematical and Theoretical

J. Phys. A: Math. Theor. **40** (2007) 8585–8598 doi:10.1088/1751-8113/40/29/026

Anisotropic pressure molecular dynamics for atomic fluid systems

M Romero-Bastida[1,3] **and R López-Rendón**[2]

[1] Facultad de Ciencias, Universidad Autónoma del Estado de Morelos, Avenida Universidad 1001, Chamilpa, Cuernavaca, Morelos 62209, Mexico
[2] Departamento de Química, Universidad Autónoma Metropolitana-Iztapalapa, Av San Rafael Atlixco 186, 09340 México DF, Mexico

E-mail: rbm@xanum.uam.mx and rlr@xanum.uam.mx

Received 2 March 2007, in final form 6 June 2007
Published 3 July 2007
Online at stacks.iop.org/JPhysA/40/8585

Abstract

The MTK equations (Martyna G J, Tobias D J and Klein M L 1994 *J. Chem. Phys.* **101** 4177–89), which simulate the constant-pressure, constant-temperature *NPT* ensemble, have been modified to simulate an anisotropic pressure along a single coordinate axis, thus rendering the $NP_{zz}T$ ensemble. The necessary theory of non-Hamiltonian systems is briefly reviewed in order to analytically prove that the proposed equations indeed sample the desired ensemble. A previously derived geometric integrator for the MTK equations is modified to take into account the anisotropic pressure and volume fluctuations. We choose a Lennard-Jones fluid as an illustrative example. The density distribution function, as well as various thermodynamic and interfacial properties of the model system in a liquid–vapour coexistence state, was computed to test the robustness of the proposed equations of motion to simulate the $NP_{zz}T$ ensemble.

PACS numbers: 05.20.−y, 02.40.−k, 31.15.Qg

1. Introduction

The extension of the methods of molecular dynamics (MD) to simulate statistical ensembles different from the microcanonical (constant energy and volume) was pioneered by Andersen [1], who proposed a constant-pressure method in which the volume was allowed to fluctuate, its average value being determined by the balance between the internal stresses in a system and the externally set pressure. This proposal initiated the 'extended phase-space' approach in which the physical coordinates and momenta are supplemented by additional variables which

[3] Also at Departamento de Física, Universidad Autónoma Metropolitana Iztapalapa, Apartado Postal 55-534, Distrito Federal 09340, Mexico.

regulate the fluctuations in the estimators that determine the thermodynamic control variables of a given statistical ensemble. By introducing additional (thermostat) variables to control the kinetic energy fluctuations [2], a unified scheme to simulate the constant-temperature, constant-pressure ensemble *NPT* by means of molecular dynamics is obtained [3].

Notwithstanding the importance of the *NPT* ensemble in numerical simulations, further developments are needed, since the isotropic volume variations inherent to the isothermal–isobaric MD approach are somewhat restrictive for certain types of physical systems of interest. So, Parrinello and Rahman extended Andersen's method to allow the MD simulation cell to change its shape; in this way they were able to explore the structural phase transitions in crystalline structures [4]. In fluid systems, the anisotropic volume fluctuations along a single coordinate axis, the z-direction, which in turn entail an applied anisotropic external pressure P_{zz}, are important in the simulation of liquid–vapour or liquid–liquid interfaces [5]. For these last two situations it would be highly desirable to develop a methodology to simulate the $NP_{zz}T$ ensemble, which would correspond to the aforementioned physical conditions. Furthermore, such methodology could offer an alternative way to study, by means of a pure MD algorithm, certain dynamical processes such as the swelling of hydrated clay–colloid systems [6], which are often simulated using hybrid Monte Carlo methods [7].

Of the various dynamical schemes already proposed to simulate the *NPT* ensemble [8–12] that can be modified in order to obtain equations of motion compatible with the $NP_{zz}T$ ensemble, we select the so-called MTK equations [13]. Our main reason is that it has been rigorously shown that they correctly reproduce the isothermal–isobaric ensemble [14] by means of a very general methodology for which a formalism has been proposed [15]. Furthermore, recently a new measure-preserving reversible geometric integrator has been developed for the MTK equations, which can be readily adapted to those corresponding to the $NP_{zz}T$ ensemble [16].

It is to be observed that extended systems are characterized by a non-Hamiltonian dynamics, but so far no general agreement has been reached as to the proper way to build a statistical mechanical theory of non-Hamiltonian systems (see [17] and references therein for a review of its connection with dynamical systems theory). In particular, certain features of the aforementioned formulation have been questioned [18, 19]. In [20], it has been attempted to build a link between the 'metric' formalism of [15] and an alternative approach that uses generalized antisymmetric brackets to define the non-Hamiltonian equations of motion [21]. Furthermore, our proposed equations to sample the $NP_{zz}T$ ensemble can be recast in a form in which they could be treated by the latter approach [22]. In any way, our main results are largely independent of the debated issues of the formalism herein adopted.

The paper is organized as follows. In section 2, we will present the necessary theory of non-Hamiltonian systems needed to build the $NP_{zz}T$ ensemble. The proposed equations of motion, together with the demonstration that they actually generate the corresponding statistical distribution, will be presented in section 3. Section 4 is devoted to modify the geometrical integrator for the *NPT* ensemble to cope with our proposed dynamical equations. In section 5, we will test our methodology by simulating an atomic Lennard-Jones fluid. Section 6 is devoted to our comments and conclusions.

2. Statistical analysis of non-Hamiltonian dynamical systems

As already mentioned in the introduction, the adopted formalism provides a framework for analysing non-Hamiltonian systems and determining the precise phase-space distribution generated by the equations of motion, assuming ergodicity. The essential details necessary to

develop the methodology to test if the proposed equations of motion indeed sample the $NP_{zz}T$ ensemble are reviewed below.

Consider a general dynamical system described by the equations of motion:

$$\dot{\mathbf{\Gamma}} = \mathbf{G}(\mathbf{\Gamma}), \tag{1}$$

where $\mathbf{\Gamma} \equiv \mathbf{\Gamma}(t)$ is the complete phase-space vector and $\mathbf{G}(\mathbf{\Gamma})$ is a vector field on the phase space which is a unique solution to equations (1) starting from an initial condition $\mathbf{\Gamma}_0$. The solution $\mathbf{\Gamma}$ can be considered as a transformation from the phase-space coordinates $\mathbf{\Gamma}_0$ at time t_0 to a new set of coordinates $\mathbf{\Gamma}$ at time t, which has a Jacobian given by $J(\mathbf{\Gamma}; \mathbf{\Gamma}_0) = |\partial\mathbf{\Gamma}/\partial\mathbf{\Gamma}_0|$. Thus, the initial phase-space volume element $\mathbf{\Gamma}_0$ transforms, under equations (1), as

$$\mathrm{d}\mathbf{\Gamma} = J(\mathbf{\Gamma}; \mathbf{\Gamma}_0)\,\mathrm{d}\mathbf{\Gamma}_0. \tag{2}$$

It has been shown [23, 15] that the Jacobian satisfies an equation of motion of the form

$$\frac{\mathrm{d}}{\mathrm{d}t} J(\mathbf{\Gamma}; \mathbf{\Gamma}_0) = \kappa(\mathbf{\Gamma}) J(\mathbf{\Gamma}; \mathbf{\Gamma}_0) \tag{3}$$

with the initial condition $J(\mathbf{\Gamma}_0; \mathbf{\Gamma}_0) = 1$. The quantity

$$\kappa(\mathbf{\Gamma}) = \nabla \cdot \mathbf{\Gamma} = \nabla \cdot \mathbf{G}(\mathbf{\Gamma}) \tag{4}$$

is known as the *compressibility* of the dynamical system, with ∇ being the gradient operator in the phase-space coordinates.

Now, a sufficient, but not necessary, condition to determine if the equations of motion are non-Hamiltonian is that $\kappa \neq 0$. From this property a number of important consequences can be derived, as will be readily shown. Equation (3) has the formal solution

$$J(\mathbf{\Gamma}; \mathbf{\Gamma}_0) = \exp\left[\int_0^t \mathrm{d}s\, \kappa(\mathbf{\Gamma}(s))\right] \equiv \exp[\omega(\mathbf{\Gamma}, t)]. \tag{5}$$

Since $\kappa(\mathbf{\Gamma}) = \mathrm{d}\ln J(\mathbf{\Gamma}; \mathbf{\Gamma}_0)/\mathrm{d}t$, it follows from equation (5) that

$$J(\mathbf{\Gamma}; \mathbf{\Gamma}_0) = \mathrm{e}^{\omega(\mathbf{\Gamma}, t) - \omega(\mathbf{\Gamma}_0, 0)}. \tag{6}$$

Substituting equation (6) into equation (2) yields

$$\mathrm{e}^{-\omega(\mathbf{\Gamma}, t)}\mathrm{d}\mathbf{\Gamma} = \mathrm{e}^{-\omega(\mathbf{\Gamma}_0, 0)}\mathrm{d}\mathbf{\Gamma}_0. \tag{7}$$

Hitherto it has not been necessary to introduce an explicit metric; the Jacobian J describes all the *geometric* effects of the transformation of coordinates. However, since for the particular ensemble to be treated in the following section a compressibility is indeed present, the factor $\exp[-\omega(\mathbf{\Gamma}, t)]$ in equation (7) can be considered as a metric determinant factor $\sqrt{g(\mathbf{\Gamma}, t)}$, where $g(\mathbf{\Gamma}, t)$ is the determinant of a metric tensor describing the geometry of phase space. Equation (7) also shows that $\exp[-\omega(\mathbf{\Gamma}, t)]\mathrm{d}\mathbf{\Gamma}$ is an invariant volume form on the manifold and, by extension, an invariant measure. The existence of this invariant measure has a number of important consequences that were pointed out in [15]. It suggests that there is an underlying fixed manifold with possibly nontrivial curvature for which the metric is determined by the compressibility. It also means that the phase-space average of some property, expressed in terms of an integral over the manifold, can be related to the time average of the same property over the trajectory generated by equations (1) under the usual assumption of ergodicity. Since the system that will be considered in the present study involves a metric factor that depends only on the phase-space coordinates $\mathbf{\Gamma}$, with no explicit time dependence, we will take $\sqrt{g(\mathbf{\Gamma})}$ without any loss of generality. The volume conservation law equation (7) can be rewritten in terms of the metric factor as

$$\sqrt{g(\mathbf{\Gamma})}\,\mathrm{d}\mathbf{\Gamma} = \sqrt{g(\mathbf{\Gamma}_0)}\,\mathrm{d}\mathbf{\Gamma}_0. \tag{8}$$

Having thus defined the volume element in phase space and the particular functional form for $\sqrt{g(\mathbf{\Gamma})}$, it becomes possible to define a probability density per unit volume $f(\mathbf{\Gamma}, t)$ in such a way that $I_{\mathcal{V}} = \int_{\mathcal{V}} \mathrm{d}\mathbf{\Gamma}\sqrt{g}\, f$ is the fraction of systems in the ensemble lying within any given region $\mathcal{V}$ of phase space at time t. Moreover, if equations (1) possess N_c conservation laws of the form $\Lambda_k(\mathbf{\Gamma}) = C_k, k = 1, \ldots, N_c$, then *all* linearly dependent variables, such as the centre-of-mass motion, must be eliminated from the dynamics by a transformation $\mathbf{\Gamma} \to \mathbf{\Gamma}'$, since the aforementioned probability density is in no way affected by them. So, as far as the dynamics described by equations (1) is ergodic, the microcanonical partition function can be constructed using

$$\Omega(C_1, \ldots, C_{N_c}) = \int_{\mathcal{V}} \mathrm{d}\mathbf{\Gamma}'\sqrt{g(\mathbf{\Gamma}')}\prod_{k=1}^{N_c}\delta(\Lambda_k(\mathbf{\Gamma}') - C_k). \tag{9}$$

Since in the present communication we are dealing with a system with an extended phase space, involving the physical system variables and additional extended variables, then equation (9) must be integrated over the extended phase-space variables in order to determine the phase-space distribution sampled by the physical variables, which must correspond to the desired statistical ensemble. The above methodology was applied in [14] to the Hoover equations of motion proposed to generate the *NPT* ensemble [9, 10] and it was shown that when $\sum_i \mathbf{F}_i = 0$ (the most common situation in MD simulations) the volume distribution is independent of the potential. On the contrary, in that same reference it was corroborated that the MTK equations, under suitable modifications to be described in the following section, correctly generate the isothermal–isobaric ensemble.

The above formalism defines the main elements needed to test whether the equations of motion to be proposed in the following section will actually generate the desired $NP_{zz}T$ ensemble.

3. The MTK equations for the $NP_{zz}T$ ensemble

As previously mentioned, we take as a point of departure the MTK equations developed for the *NPT* ensemble in [13]. However, besides the obvious modifications that have to be incorporated to generate the $NP_{zz}T$ ensemble, the originally employed Nosé–Hoover thermostat, described in terms of a *single* extended variable, is replaced by a chain of M extended variables $\{\eta_k, p_{\eta_k}\}_{k=1}^{M}$ and another set of extended variables $\{\xi_k, p_{\xi_k}\}_{k=1}^{M}$ are coupled to the barostat. These new variables serve to drive the fluctuations of the kinetic energy and the internal pressure estimator (see below), respectively. Additional mass-like parameters, $\{Q_k\}_{k=1}^{M}$ and $\{Q'_k\}_{k=1}^{M}$, are assigned to each of these extended variables, being these parameters the ones which determine the timescales on which the latter evolve.

The usefulness of this approach, known as the Nosé–Hoover chain (NHC) method [24, 25], was exemplified in [14] by modifying the equations corresponding to the Hoover algorithm (which employs a single extended variable in its original form) with the addition of the NHC variables, and so, by applying the methodology of section 2, the serious pathology mentioned at the end of that same section is eliminated, but nevertheless a volume distribution that contains a factor inversely proportional to the volume of the system is obtained, indicating that a $(N-1)PT$ ensemble is generated. On the contrary, when the MTK equations are supplemented with the same NHC variables, the correct volume distribution of the *NPT* ensemble is indeed obtained [14]. Furthermore, an added advantage of the use of the chain variables is that is has been shown that they are helpful to improve the performance of non-equilibrium simulations. In particular, the boundary oscillators in an anharmonic lattice,

which are thermostated at different temperatures to obtain a heat flux, have the correct ergodic behaviour only if the NHC method is employed [26]. It has also been shown that for high shear rates in non-equilibrium MD simulations of liquid *n*-decane, temperature control is much harder to obtain without the use of NHC [27]. However, the lack of a corresponding non-equilibrium microcanonical ensemble prevents a rigorous extended phase-space analysis, such as that presented in section 2 corresponding to equilibrium conditions, to be performed.

3.1. Equations of motion

The proposed equations of motion have the following basic form for a d-dimensional system of N particles (N_f degrees of freedom; $N_f = dN$ for a system with no constraints):

$$\begin{aligned}
\dot{\mathbf{r}}_i &= \frac{\mathbf{p}_i}{m_i} + \frac{\widetilde{p}_\epsilon}{W_g} \cdot \mathbf{r}_i \\
\dot{\mathbf{p}}_i &= \mathbf{F}_i - \frac{\widetilde{p}_\epsilon}{W_g} \cdot \mathbf{p}_i - \frac{1}{N_f}\frac{\mathrm{Tr}[\widetilde{p}_\epsilon]}{W_g}\mathbf{p}_i - \frac{p_{\eta_1}}{Q_1}\mathbf{p}_i \\
\dot{\widetilde{h}} &= \frac{\widetilde{p}_\epsilon \cdot \widetilde{h}}{W_g} \\
\dot{\widetilde{p}}_\epsilon &= V(\widetilde{P}_{\mathrm{int}} - P_{zz}\tilde{I}) \cdot \tilde{I}_z + \left(\frac{1}{N_f}\sum_{i=1}^{N}\frac{\mathbf{p}_i^2}{m_i}\right)\tilde{I}_z - \frac{p_{\xi_1}}{Q'_1}\widetilde{p}_\epsilon \\
\dot{\eta}_k &= \frac{p_{\eta_k}}{Q_k}, \qquad k = 1, \ldots, M \\
\dot{p}_{\eta_k} &= G_k - \frac{p_{\eta_{k+1}}}{Q_{k+1}}p_{\eta_k} \\
\dot{p}_{\eta_M} &= G_M \\
\dot{\xi}_k &= \frac{p_{\xi_k}}{Q'_k}, \qquad k = 1, \ldots, M \\
\dot{p}_{\xi_k} &= G'_k - \frac{p_{\xi_{k+1}}}{Q'_{k+1}}p_{\xi_k} \\
\dot{p}_{\xi_M} &= G'_M,
\end{aligned} \tag{10}$$

where $\mathbf{F}_i = -\partial U/\partial \mathbf{r}_i$ is the force on particle i, each of mass m_i. Here, the tensorial variable $\widetilde{p}_\epsilon$, together with the mass parameter W_g, corresponds to the barostat, coupled both to the positions and the momenta. $\tilde{I}$ is the identity matrix and $\tilde{I}_z$ is a matrix such that $(\tilde{I}_z)_{zz} = 1$ and zero otherwise. The geometry of the simulation cell is defined by the matrix of cell parameters $\widetilde{h}$ which (since all the angles between the cell sides are fixed) has the explicit form

$$\widetilde{h} = \begin{pmatrix} L_x & 0 & 0 \\ 0 & L_y & 0 \\ 0 & 0 & L_z \end{pmatrix}. \tag{11}$$

Thus, the volume of the simulation cell is $V = \det[\widetilde{h}]$, which automatically satisfies the constraint $V \geqslant 0$ since $\mathrm{Tr}[\widetilde{p}_\epsilon] = W_g \mathrm{d}(\ln\det[\widetilde{h}])/\mathrm{d}t$. The imposed external pressure along the z-axis is P_{zz} and

$$(\widetilde{P}_{\mathrm{int}})_{\alpha\beta} = \frac{1}{V}\left[\sum_{i=1}^{N}\frac{(\mathbf{p}_i)_\alpha(\mathbf{p}_i)_\beta}{m_i} + \sum_{i=1}^{N}(\mathbf{r}_i)_\alpha(\mathbf{F}_i)_\beta - (\widetilde{U}'\widetilde{h}^T)_{\alpha\beta}\right], \tag{12}$$

together with $(U')_{\alpha\beta} = \partial U(\mathbf{r}, \widetilde{h})/\partial(\widetilde{h})_{\alpha\beta}$, is the internal pressure estimator. Since the barostat tends to evolve on a much slower timescale than that corresponding to the particles, we have

coupled two Nosé–Hoover chains to the system, one to the particle coordinates and the other to the barostat. The heat-bath 'forces' which drive the time evolution of the thermostat variables $\{\eta_k, p_{\eta_k}\}$ are given by

$$G_1 = \sum_{i=1}^{N} \frac{\mathbf{p}_i^2}{m_i} - N_f k_B T, \qquad G_k = \frac{p_{\eta_{k-1}}^2}{Q_{k-1}} - k_B T, \tag{13}$$

whereas the extended forces G'_k associated with the chain variables $\{\xi_k, p_{\xi_k}\}$ coupled to the barostat are defined by

$$G'_1 = \frac{\mathrm{Tr}\,[\widetilde{p}_\epsilon \widetilde{p}_\epsilon{}^T]}{W_g} - k_B T, \qquad G'_k = \frac{p_{\xi_{k-1}}^2}{Q'_{k-1}} - k_B T. \tag{14}$$

Equations (10) have the conserved variable

$$H' = H(\mathbf{p}, \mathbf{r}) + \frac{\mathrm{Tr}[\widetilde{p}_\epsilon \widetilde{p}_\epsilon{}^T]}{2W_g} + P_{zz} \det[\widetilde{h}] + \sum_{k=1}^{M} \left(\frac{p_{\eta_k}^2}{2Q_k} + \frac{p_{\xi_k}^2}{2Q'_k} \right)$$
$$+ 3Nk_B T \eta_1 + k_B T \eta_c + k_B T \sum_{k=1}^{M} \xi_k, \tag{15}$$

where $\eta_c = \sum_{k=2}^{M} \eta_k$. In order to prove that the MTK equations generate a correct isothermal–isobaric distribution, one has to substitute the constants derived from the conservation laws and compatible with equations (10), together with the corresponding metric, into equation (9) and perform the integrals over all the extended variables, following the same procedure that was applied both to the canonical and isothermal–isobaric ensembles [14].

3.2. The partition function of the $NP_{zz}T$ ensemble

In order to simplify the foregoing analysis, the particles and the barostat will be coupled to the *same* Nosé–Hoover chain thermostat. Now, according to the procedure of section 2, the driven and linearly dependent variables must be eliminated in order to perform a proper formal analysis. Since we are considering the case in which there are no external forces on the system, that is $\sum_i \mathbf{F}_i = 0$, then, according to Nosé, there are d additional conservation laws satisfied by equations (10) which take the form $\mathbf{P}(\det[\widetilde{h}]^{1/N_f} \mathrm{e}^{\eta_1}) = \mathbf{K}$, where $\mathbf{P} = \sum_{i=1}^{N} \mathbf{p}_i$ is the centre-of-mass momentum of the system and $\mathbf{K}$ is an arbitrary vector in d dimensions. It can be easily verified that there is just one independent component of $\mathbf{P}$, which we take, without loss of generality, to be $\mathcal{P}_z$. Thus, $d-1$ components of the centre-of-mass momenta must be eliminated. This step is accomplished by a canonical transformation to a set of relative coordinates and momenta $\{\mathbf{p}', \mathcal{P}_z, \mathbf{r}', \mathcal{R}_z\}$. This procedure yields the following transformed equations of motion:

$$\dot{\mathbf{r}}'_i = \frac{\mathbf{p}'_i}{m_i} + \frac{\widetilde{p}_\epsilon}{W_g} \cdot \mathbf{r}'_i$$
$$\dot{\mathbf{p}}'_i = \mathbf{F}'_i - \frac{\widetilde{p}_\epsilon}{W_g} \cdot \mathbf{p}'_i - \frac{1}{N_f} \frac{\mathrm{Tr}[\widetilde{p}_\epsilon]}{W_g} \mathbf{p}'_i - \frac{p_{\eta_1}}{Q_1} \mathbf{p}'_i$$
$$\dot{\mathcal{P}}_z = -\left(1 + \frac{1}{N_f}\right) \frac{p_\epsilon^{zz}}{W_g} \mathcal{P}_z - \frac{p_{\eta_1}}{Q_1} \mathcal{P}_z$$
$$\dot{\widetilde{h}} = \frac{\widetilde{p}_\epsilon \cdot \widetilde{h}}{W_g}$$

$$\begin{aligned}
\dot{\widetilde{p}}_\epsilon &= V(\widetilde{P}_{\rm int} - P_{zz}\tilde{I})\cdot\tilde{I}_z + \frac{1}{N_f}\left(\sum_{i=1}^{N-1}\frac{(p'_{iz})^2}{m_i} + \frac{\mathcal{P}_z^2}{\mathcal{M}}\right)\tilde{I}_z - \frac{p_{\eta_1}}{Q_1}\widetilde{p}_\epsilon \\
\dot{\eta}_k &= \frac{p_{\eta_k}}{Q_k}, \qquad k = 1,\ldots,M \\
\dot{p}_{\eta_1} &= \sum_{i=1}^{N-1}\frac{(p'_{iz})^2}{m_i} + \frac{\mathcal{P}_z^2}{\mathcal{M}} + \frac{{\rm Tr}\left[\widetilde{p}_\epsilon\widetilde{p}_\epsilon{}^T\right]}{W_g} - Lk_BT - \frac{p_{\eta_2}}{Q_2}p_{\eta_1} \\
\dot{p}_{\eta_k} &= \frac{p^2_{\eta_{k-1}}}{Q_{k-1}} - k_BT - \frac{p_{\eta_{k+1}}}{Q_{k+1}}p_{\eta_k} \\
\dot{p}_{\eta_M} &= \frac{p^2_{\eta_{M-1}}}{Q_{M-1}} - k_BT,
\end{aligned} \tag{16}$$

where $\mathcal{M}$ is the total mass of the system and the parameter L will be determined in the analysis. These equations have a phase-space metric factor

$$\sqrt{g(\mathbf{\Gamma})} = \frac{1}{\det[\widetilde{h}]^{(d/N_f-1-1/N_f)}}\exp([d(N-1)+2]\eta_1 + \eta_c), \tag{17}$$

as well as two conserved quantities,

$$\Lambda_1(\mathbf{\Gamma}) = H(\mathbf{p}',\mathbf{r}',\mathcal{P}_z) + \frac{{\rm Tr}[\widetilde{p}_\epsilon\widetilde{p}_\epsilon{}^T]}{W_g} + \sum_{k=1}^{M}\frac{p^2_{\eta_k}}{2Q_k} + Lk_BT\eta_1 + k_BT\eta_c + P_{zz}\det[\widetilde{h}] \tag{18}$$

and

$$\Lambda_2(\mathbf{\Gamma}) = \mathcal{P}_z\det[\widetilde{h}]^{1/N_f}\exp\eta_1. \tag{19}$$

Note the fact that $H(\mathbf{p},\mathbf{r}) \equiv H(\mathbf{p}',\mathbf{r}',\mathcal{P}_z)$ has been employed.

The conservation laws and the metric can now be used to construct the microcanonical partition function, by means of equation (9), as

$$\begin{aligned}
\Omega_{T,P_{zz}}(N,C_1,C_2) = &\int {\rm d}\widetilde{h}\int {\rm d}\mathcal{P}_z\int {\rm d}^{N-1}\mathbf{p}'\int {\rm d}^{N-1}\mathbf{r}'\int {\rm d}\eta_1{\rm d}\eta_c{\rm d}^M p_\eta\,{\rm d}p_\epsilon^{zz} \\
&\times\frac{1}{\det[\widetilde{h}]^{(d/N_f-1-1/N_f)}}\exp([d(N-1)+2]\eta_1+\eta_c) \\
&\times\delta\left(H(\mathbf{p}',\mathcal{P}_z,\mathbf{r}') + \frac{\left(p_\epsilon^{zz}\right)^2}{2W_g} + \sum_{k=1}^{M}\frac{p^2_{\eta_k}}{2Q_k} + Lk_BT\eta_1 + k_BT\eta_c + P_{zz}\det[\widetilde{h}] - C_1\right) \\
&\times\delta(\mathcal{P}_z\det[\widetilde{h}]^{1/N_f}\exp\eta_1 - C_2).
\end{aligned} \tag{20}$$

The distribution function in the physical subspace is obtained by integrating over η_1 and η_c. Performing the first integration, we obtain

$$\begin{aligned}
\Omega_{T,P_{zz}}(N,C_1,C_2) = &\frac{1}{|C_1|}\int {\rm d}\widetilde{h}\int {\rm d}\mathcal{P}_z\int {\rm d}^{N-1}\mathbf{p}'\int {\rm d}^{N-1}\mathbf{r}'\int {\rm d}\eta_c\,{\rm d}^M p_\eta\,{\rm d}p_\epsilon^{zz} \\
&\times\frac{1}{\det[\widetilde{h}]^{(d/N_f-1-1/N_f)}}\exp(\eta_c)\left(\frac{C_2}{\mathcal{P}_z\det[\widetilde{h}]^{1/N_f}}\right)^{N_f-d-2} \\
&\times\delta\left(H(\mathbf{p}',\mathcal{P}_z,\mathbf{r}') + \frac{\left(p_\epsilon^{zz}\right)^2}{2W_g} + \sum_{k=1}^{M}\frac{p^2_{\eta_k}}{2Q_k} + Lk_BT\eta_1 + k_BT\eta_c + P_{zz}\det[\widetilde{h}] - C_1\right).
\end{aligned} \tag{21}$$

The next step is to perform the integration over η_c and making the identification $L = N_f + 1$, rendering the final form of the partition function as

$$\Omega_{T,P_{zz}}(N, C_1, C_2) = \frac{\beta \exp(\beta C_1)}{C_2^d} \left\{ \prod_{k=1}^{M} \int \mathrm{d}p_{\eta_k} \exp\left(-\beta \frac{p_{\eta_k}^2}{2Q_k} \right) \right\} \int \mathrm{d}p_\epsilon^{zz} \exp\left(-\beta \frac{\left(p_\epsilon^{zz}\right)^2}{2W_g} \right)$$
$$\times \int \mathrm{d}\widetilde{h} \int \mathrm{d}\mathcal{P}_z \int \mathrm{d}^{N-1}\mathbf{p}' \int \mathrm{d}^{N-1}\mathbf{r}' \mathcal{P}_z^{d-1} \det[\widetilde{h}] \exp(-\beta P_{zz} \det[\widetilde{h}])$$
$$\times \exp(-\beta H(\mathbf{p}', \mathcal{P}_z, \mathbf{r}')). \tag{22}$$

Thus, it is clear that the modified MTK equations will generate the desired $NP_{zz}T$ ensemble for the conditions more usually employed in MD simulations.

4. Geometric integration and the Liouville operator

The approach that will be employed to integrate the $NP_{zz}T$ equations of motion is based on the general methodology to develop geometric integrators of non-Hamiltonian systems, based upon a generalization of the Liouville operator. The use of this technique, first introduced in [28], has been further refined and later applied to integrate the equations of motion for the *NPT* ensemble [16]. This methodology will thus be adopted to develop the integrator corresponding to the equations of motion of the $NP_{zz}T$ ensemble. Before discussing this case, however, let us first review briefly the fundamental concepts.

The equations of motion, equation (1), can be written in the form of an operator equation

$$\dot{\mathbf{\Gamma}} = \mathrm{i}L\mathbf{\Gamma}, \tag{23}$$

where

$$\mathrm{i}L = \mathbf{G}(\mathbf{\Gamma}) \cdot \nabla \tag{24}$$

is a generalization of the Liouville operator and $\mathbf{\Gamma}(t)$ is a point in the extended phase-space defined by

$$\mathbf{\Gamma}(t) = \left\{ \mathbf{r}, \mathbf{p}; \{\eta_k\}_{k=1}^M, \left\{p_{\eta_k}\right\}_{k=1}^M, \{\xi_k\}_{k=1}^M, \left\{p_{\xi_k}\right\}_{k=1}^M \right\}. \tag{25}$$

When the equations of motion are expressed as in equation (23), the evolution of an arbitrary initial condition $\mathbf{\Gamma}_0$ can be determined formally according to

$$\mathbf{\Gamma} = \mathrm{e}^{\mathrm{i}Lt}\mathbf{\Gamma}_0, \tag{26}$$

where the operator $\exp(\mathrm{i}Lt)$ is known as the classical propagator. Although equation (26) is only a formal solution, it is, nevertheless, the starting point for the development of geometrical integration schemes.

Integrating the equations of motion (10) is a straightforward generalization of the method already developed in [16] for those corresponding to the *NPT* ensemble, with only minor modifications that will be readily described. From $\widetilde{p}_\epsilon = W_g \dot{\widetilde{h}} \widetilde{h}^{-1} \equiv W_g \dot{\widetilde{\epsilon}}$, with $(\dot{\widetilde{\epsilon}})_{zz} = \dot{\epsilon}_{zz}$ and zero otherwise, we obtain the scalar equation $p_\epsilon^{zz} = W_g \dot{\epsilon}_{zz}$, which will be integrated instead of the third equation in (10). Since only L_z changes, the variable $\epsilon_{zz} = \ln(L_z/L_z^0)$ can be readily defined.

The total Liouville operator in equation (26) can be separated as

$$\mathrm{i}L = \mathrm{i}L_1 + \mathrm{i}L_2 + \mathrm{i}L_\epsilon + \mathrm{i}L_{p_\epsilon^{zz}} + \mathrm{i}L_\mathrm{B} + \mathrm{i}L_\mathrm{T}, \tag{27}$$

where

$$\begin{aligned}
\mathrm{i}L_1 &= \sum_{i=1}^{N}\left[\frac{\mathbf{p}_i}{m_i}+\frac{p_\epsilon^{zz}}{W_g}\mathbf{r}_i\right]\cdot\frac{\partial}{\partial\mathbf{r}_i}\\
\mathrm{i}L_2 &= \sum_{i=1}^{N}\left[\mathbf{F}_i-\alpha\frac{p_\epsilon^{zz}}{W_g}\mathbf{p}_i\right]\cdot\frac{\partial}{\partial\mathbf{p}_i}\\
\mathrm{i}L_\epsilon &= \frac{p_\epsilon^{zz}}{W_g}\frac{\partial}{\partial\epsilon_{zz}}\\
\mathrm{i}L_{p_\epsilon^{zz}} &= G_\epsilon\frac{\partial}{\partial p_\epsilon^{zz}}\\
\mathrm{i}L_{\mathrm{T}} &= \sum_{k=1}^{M}\left[\frac{p_{\eta_k}}{Q_k}\frac{\partial}{\partial\eta_k}+G_k\frac{\partial}{\partial p_{\eta_k}}\right]-\sum_{i=1}^{N}\frac{p_{\eta_1}}{Q_1}\mathbf{p}_i\cdot\frac{\partial}{\partial\mathbf{p}_i}-\sum_{k=1}^{M-1}\frac{p_{\eta_{k+1}}}{Q_{k+1}}p_{\eta_k}\frac{\partial}{\partial p_{\eta_k}},
\end{aligned}\tag{28}$$

with $\alpha = 1 + 1/N_f$ and

$$G_\epsilon = \alpha\sum_{i=1}^{N}\frac{p_{iz}^2}{m_i}+\sum_{i=1}^{N}z_i F_{iz} - P_{zz}V.\tag{29}$$

The remaining operator $\mathrm{i}L_{\mathrm{B}}$, which corresponds to the chain variables coupled to the barostat, is defined in an analogous manner to the operator $\mathrm{i}L_{\mathrm{T}}$ in (28) which defines the thermostat, but written instead in terms of the variables $\{\xi_k, p_{\xi_k}\}$ and the set $\{Q_k'\}$ of the mass-like parameters.

The classical propagator in (26) has to be factorized in a symmetric form that ensures that the resulting integrator will be both symplectic and time reversible. Now, for a small time interval Δt, a Trotter factorization along the route shown in [28] leads to an approximate propagator of the form

$$\begin{aligned}
\exp(\mathrm{i}L\Delta t) = {}& \exp\left(\mathrm{i}L_{\mathrm{B}}\frac{\Delta t}{2}\right)\exp\left(\mathrm{i}L_{\mathrm{T}}\frac{\Delta t}{2}\right)\exp\left(\mathrm{i}L_{p_\epsilon^{zz}}\frac{\Delta t}{2}\right)\exp\left(\mathrm{i}L_2\frac{\Delta t}{2}\right)\\
&\times\exp(\mathrm{i}L_\epsilon\Delta t)\exp(\mathrm{i}L_1\Delta t)\exp\left(\mathrm{i}L_2\frac{\Delta t}{2}\right)\exp\left(\mathrm{i}L_{p_\epsilon^{zz}}\frac{\Delta t}{2}\right)\\
&\times\exp\left(\mathrm{i}L_{\mathrm{T}}\frac{\Delta t}{2}\right)\exp\left(\mathrm{i}L_{\mathrm{B}}\frac{\Delta t}{2}\right)+\mathcal{O}(\Delta t^3).
\end{aligned}\tag{30}$$

By means of the *direct translation* technique [29], each operator in the above expression can be directly 'translated' into the lines of a computer code. To decompose the action of the operators $\exp(\mathrm{i}L_{\mathrm{B}}\Delta t/2)$ and $\exp(\mathrm{i}L_{\mathrm{T}}\Delta t/2)$ in order to guarantee a driftless value of the constant of motion, the higher order Suzuki–Yoshida factorization is applied [30, 31]. The way in which this factorization is applied to the operators corresponding to the NHC equations has been thoroughly discussed in [16]. All the ensuing elementary operators that result after the Suzuki–Yoshida decomposition is applied are either translation or scaling operators,

$$\exp\left(c\frac{\partial}{\partial y}\right)f(y) = f(y+c),\qquad \exp\left(cx\frac{\partial}{\partial x}\right)x = x\exp(c).\tag{31}$$

The operators $\exp(\mathrm{i}L_\epsilon\Delta t)$ and $\exp(\mathrm{i}L_{p_\epsilon^{zz}}\Delta t/2)$ are simple translation operators. The operators $\exp(\mathrm{i}L_1\Delta t)$ and $\exp(\mathrm{i}L_2\Delta t/2)$ are somewhat more complicated than their microcanonical or canonical ensemble counterparts due to the barostat coupling. The action of the operator $\exp(\mathrm{i}L_1\Delta t)$, which results in an evolution equation for the positions, has already been determined [29], and yields

$$\mathbf{r}_i(\Delta t) = \mathbf{r}_i(0)\,\mathrm{e}^{p_\epsilon^{zz}\Delta t/W_g}+\Delta t\frac{\mathbf{p}_i(0)}{m_i}\,\mathrm{e}^{p_\epsilon^{zz}\Delta t/2W_g}\frac{\sinh\left(p_\epsilon^{zz}\Delta t/2W_g\right)}{p_\epsilon^{zz}\Delta t/2W_g}\tag{32}$$

for an arbitrary initial condition $\{\mathbf{r}_i(0), \mathbf{p}_i(0)\}$ and a constant p_ϵ. Similarly, the action of $\exp(iL_2\Delta t/2)$, for the initial values $\{\mathbf{p}_i(0)\}$ and $\{\mathbf{F}_i(0)\}$, results in

$$\mathbf{p}_i(\Delta t/2) = \mathbf{p}_i(0)\,\mathrm{e}^{-\alpha p_\epsilon^{zz}\Delta t/2W_g} + \frac{\Delta t}{2}\mathbf{F}_i(0)\,\mathrm{e}^{-\alpha p_\epsilon^{zz}\Delta t/4W_g}\frac{\sinh\left(\alpha p_\epsilon^{zz}\Delta t/4W_g\right)}{\alpha p_\epsilon^{zz}\Delta t/4W_g}. \tag{33}$$

It is to be observed that the potentially singular factor $\sinh(x)/x$ should be evaluated by means of a power series for small x to avoid numerical instabilities in practical implementations. These equations, together with the Suzuki–Yoshida factorization of the thermostat and barostat operators, completely define an integrator for which it has already been shown to reproduce correctly the $NP_{zz}T$ ensemble.

5. An example of the $NP_{zz}T$ equations of motion

5.1. Simulation details

In order to illustrate the proposed equations of motion for the $NP_{zz}T$ ensemble, we performed molecular dynamics simulations on the liquid–vapour interface of a simple Lennard-Jones (LJ) fluid. Reduced units were employed throughout the work. A single barostat was employed to control the pressure fluctuations, whereas a separate NHC thermostat was coupled to each fluid particle. It has been shown elsewhere [2, 11] that each of the mass-like thermostat and barostat parameters $\{Q_\alpha\}$ and $\{Q'_\alpha\}$, as well as W_g, should be

$$\begin{aligned} Q_1 &= dk_B T\tau_T^2, & Q_k &= k_B T\tau_T^2, \\ Q'_1 &= d^2 k_B T\tau_B^2, & Q'_k &= k_B T\tau_B^2, \\ W_g &= (N_f+1)k_B T\tau_B^2, \end{aligned} \tag{34}$$

where τ_B and τ_T are the barostat and thermostat response times, respectively. A NHC length of $M = 4$ was chosen for all simulations. The employed temperatures were taken in a range from $T^* = 0.8$ to 1.2, whereas the pressure was varied from $P^* = 0.004$ to 0.07. For this range of values the system is in a liquid–vapour coexistence state. Therefore, to prepare the initial configuration for each temperature, a dense slab of $N = 1372$ unit mass atoms was placed in the middle of the simulation cell along the z-direction. Such setting allowed us to obtain two free liquid–vapour interfaces perpendicular to the z-axis. Periodic boundary conditions and the minimum image convention were applied in all directions. The LJ potential was truncated at a cut-off radius of $r_c^* = 4.0$ in order to minimize the truncation effects. Equilibration was attained after 5×10^5 time steps, and all the equilibrium properties were obtained from a trajectory computed for an additional number 10^6 of time steps. The time-step value was $\Delta t^* = 0.003$ in all simulations. The vapour pressure was obtained as the average normal component of the pressure to the liquid–vapour interface $\langle P_{zz}^*\rangle$, with $\langle\cdots\rangle$ being the time average. The surface tension γ^* was computed using the average normal and tangential components of the pressure to the interfaces as

$$\gamma^* = \frac{L_z^*}{2}\left[\langle P_{zz}^*\rangle - \frac{1}{2}(\langle P_{xx}^*\rangle + \langle P_{yy}^*\rangle)\right], \tag{35}$$

where L_z^* is the simulation box length in the z-direction and the factor $1/2$ is due to the existence of two liquid–vapour interfaces in the system.

5.2. Results

In figure 1(*a*), we present the results for the density distribution function computed for the thermodynamic state corresponding to $T^* = 1.2$ and $P_{zz}^* = 0.07$. Since the timescales

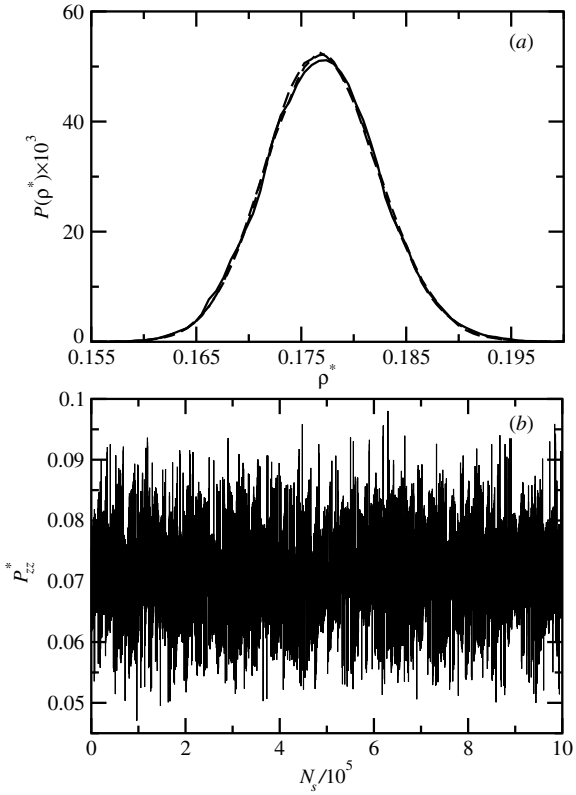

Figure 1. (*a*) Density distribution function of the LJ fluid for $T^* = 1.2$ and $P^*_{zz} = 0.07$ and the following sets of thermostat and barostat response times: (i) $\tau_T = 0.01, \tau_B = 0.1$ (solid curve), (ii) $\tau_T = 0.1, \tau_B = 0.01$ (dashed curve) and (iii) $\tau_T = 5.0, \tau_B = 0.01$ (long dashed curve). (*b*) P^*_{zz} as a function of the number N_s of time steps.

associated to the thermostat are much shorter than those corresponding to the barostat, $\tau_T < \tau_B$, we chose $\tau_T = 0.01$ and $\tau_B = 0.1$ as the first set of values. For this case it is seen that the shape of the distribution is, to a large extent, Gaussian, which is consistent with the results of section 3. Two further sets of response times are given in the same figure: one in which the aforementioned values of τ_T and τ_B are interchanged and other in which τ_T takes a rather large value while keeping τ_B small. As can be readily seen, the resulting differences are negligible. We also evaluated the error in the conserved quantity equation (15), which is defined as $\Delta E = N_s^{-1} \sum_i |(E_i - E_0)/E_0|$, where i runs over the number N_s of time steps. For the first set of response time values reported in figure 1(*a*), the computed error has a value of $\Delta E = 4.18 \times 10^{-5}$, being of the same order for the other reported sets. No drift in the conserved quantity was observed, even if a shorter time step of $\Delta t^* = 0.001$ is employed instead. Furthermore, no dependence on the integration time-step value was detected on the computed quantities. For these, their fluctuations are always around a mean value which closely corresponds to the external imposed value, as can be readily seen in the time evolution of the instantaneous value of P^*_{zz} depicted in figure 1(*b*). The average temperature and pressure values obtained are $\langle T^* \rangle = 1.20 \pm 0.03$ and $\langle P^*_{zz} \rangle = 0.069 \pm 0.006$, in excellent agreement with the imposed values.

Figure 2 presents the results of $\ln P^*_{zz}$ against $1/T^*$ for the aforementioned ranges of temperatures and pressures, and with the parameter set $(\tau_T, \tau_B) = (0.01, 0.1)$. In this case,

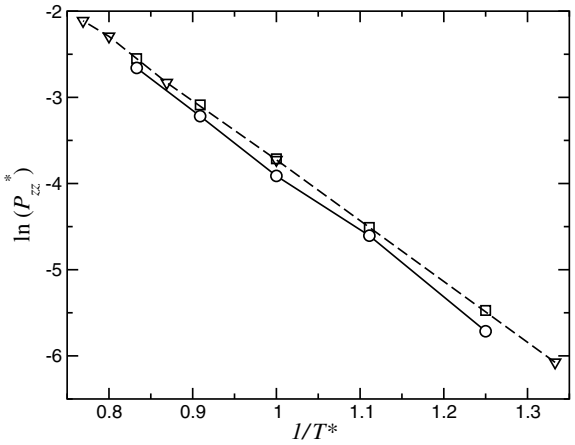

Figure 2. P^*_{zz} versus temperature T^*. The results of this work (circles), with $N = 1372$ and $(\tau_T, \tau_B) = (0.01, 0.1)$, are compared with those of [32] (squares), which correspond to a *NVT* simulation, and [33], which were computed by means of the Gibbs ensemble Monte Carlo method. The maximum standard deviation is $\mathcal{O}(10^{-3})$ for all data points and the lines are drawn to guide the eye.

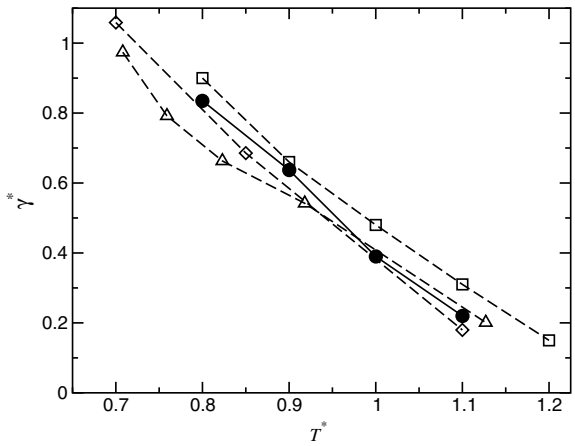

Figure 3. Surface tension γ^* versus temperature T^*. The results of this work (filled circles), with $N = 1372$ and the (τ_T, τ_B) parameters of figure 2, are compared with those of [32], (squares, $N = 2048$), [34] (diamonds, $N = 1372$) and [35] (triangles, $N = 255$); all of them correspond to *NVT* simulations with $r_c = 2.5$. The maximum standard deviation is $\mathcal{O}(10^{-2})$ for all data points and the lines are drawn to guide the eye.

P^*_{zz} corresponds to the vapour pressure of the system. We compare our results with the corresponding values obtained from a simulation in the *NVT* ensemble with $N = 1024$ and $r^*_c = 3.0$ [32], which explicitly include the liquid–vapour interfaces, as well as with those of a Gibbs ensemble Monte Carlo simulation [33], which does not include the interfaces. A good agreement with the results of these latter methodologies is indeed obtained. We also performed some simulations for $T^* > 1.2$ and $P^*_{zz} > 0.069$, above the critical point. For these thermodynamic states all the diagonal components of the pressure tensor were identical, a behaviour corresponding to a homogeneous fluid. Therefore, a correct description of phase behaviour is obtained with our methodology.

The results for the surface tension as a function of temperature are reported in figure 3. It can be observed that the γ^* values decrease monotonically with the temperature and are consistent with those of various simulations performed in the *NVT* ensemble, which are presented in that same figure for comparison. The observed differences are due to the different schemes employed in the computation of this property, as well as to the various N values used and to the ensemble in which the simulations were performed. Nevertheless, the overall agreement with the reported values in the literature is within an acceptable range, thus validating the effectiveness of our methodology to compute interfacial properties of fluid systems.

6. Conclusions

In this work, we have modified the MTK equations for the *NPT* ensemble to incorporate the anisotropic pressure fluctuations along a single direction, thus rendering the $NP_{zz}T$ ensemble. By using the formalism of [14], it has been analytically shown that the proposed equations correctly sample the desired ensemble. By means of a geometric integrator previously employed to solve the equations of the *NPT* ensemble we numerically integrated our equations and found that the correct density distribution function is indeed generated, corroborating our analytical results. Further refinements could be obtained by employing more sophisticated thermostats [36], which could improve the performance of the integrator in more demanding conditions, i.e. non-equilibrium simulations such as those mentioned in section 3. We remark that the methodology herein presented can be applied not only to MD simulations of complex molecules, for which the extension is immediate, but also to simulations employing other dynamical simulation methodologies. For example, within the scheme of the mesoscopic dissipative particle dynamics method, a Galilean-invariant Nosé–Hoover thermostat [37] has been recently implemented. Since this thermostat is a special instance of the general case discussed in [24], our proposed $NP_{zz}T$ barostat could also be readily implemented, making thus possible to simulate liquid–liquid interfaces without the necessity to employ stochastic methods to control volume fluctuations.

We want to remark that the MTK equations are not the only scheme proposed to generate the *NPT* ensemble from which the corresponding equations to simulate the anisotropic pressure fluctuations in fluid systems could be derived, as already mentioned in the introduction. In [38] an implementation of the scheme of [12], which is based on a modification of the original Andersen barostat [1], was developed employing a similar geometric integrator technique to that employed in the present work. It could be interesting to modify this proposal to incorporate an external anisotropic pressure and make a more thorough comparison of the interfacial properties computed from these two different methodologies.

Acknowledgments

We want to thank J Alejandre for useful discussions and encouragement during the first stages of this work. Financial support from Consejo Nacional de Ciencia y Tecnología (CONACyT) is also acknowledged.

References

[1] Andersen H C 1980 *J. Chem. Phys.* **72** 2384–92
[2] Nosé S 1984 *J. Chem. Phys.* **81** 511–9
[3] Nosé S 1984 *Mol. Phys.* **52** 255–68

[4] Parrinello M and Rahman A 1981 *Phys. Rev. Lett.* **45** 1196–9
[5] Zhang Y, Feller S E, Brooks B R and Pastor R W 1995 *J. Chem. Phys.* **103** 10252–66
[6] Odriozola G and Aguilar J F 2005 *J. Chem. Theory Comput.* **1** 1211–20
[7] Mehling B, Heermann D W and Forrest B M 1992 *Phys. Rev.* B **45** 679–85
[8] Nosé S and Klein M L 1983 *Mol. Phys.* **50** 1055–76
[9] Hoover W G 1985 *Phys. Rev.* A **31** 1695–97
[10] Hoover W G 1986 *Phys. Rev.* A **34** 2499–500
[11] Melchionna S, Ciccotti G and Holian B L 1993 *Mol. Phys.* **78** 533–44
[12] Ferrario M 1993 *Computer Simulation in Chemical Physics* ed M P Allen and D J Tildesley (Dordrecht: Kluwer) p 153
[13] Martyna G J, Tobias D J and Klein M L 1994 *J. Chem. Phys.* **101** 4177–89
[14] Tuckerman M E, Liu Y, Ciccotti G and Martyna G J 2001 *J. Chem. Phys.* **115** 1678–702
[15] Tuckerman M E, Mundy C J and Martyna G J 1999 *Europhys. Lett.* **45** 149–53
[16] Tuckerman M E, Alejandre J, López-Rendón R, Jochim A L and Martyna G J 2006 *J. Phys. A: Math. Gen.* **39** 5629–51
[17] Klages R 2003 *Preprint* nlin.CD/0309069
[18] Ramshaw J D 2002 *Europhys. Lett.* **59** 319–23
[19] Sergi A and Giaquinta P V 2007 *J. Stat. Mech.* P02013
[20] Tarsov V E 2005 *J. Phys. A: Math. Gen.* **38** 2145–55
[21] Sergi A 2003 *Phys. Rev.* E **67** 021101-1,7
[22] Sergi A and Ferrario M 2001 *Phys. Rev.* E **64** 056125−1,9
[23] Andrey L 1986 *Phys. Lett.* A **114** 183
[24] Martyna G J, Klein M L and Tuckerman M E 1992 *J. Chem. Phys.* **97** 2635–43
[25] Frenkel D and Smit B 2002 *Understanding Molecular Simulations: From Algorithms to Applications* 2nd edn (New York: Academic)
[26] Romero-Bastida M and Aguilar J F 2006 *J. Phys. A: Math. Gen.* **39** 11155–70
[27] Mundy C J, Siepmann J I and Klein M L 1995 *J. Chem. Phys.* **103** 10192–200
[28] Tuckerman M, Berne B J and Martyna G J 1992 *J. Chem. Phys.* **97** 1990–2001
[29] Martyna G J, Tuckerman M E, Tobias D J and Klein M L 1996 *Mol. Phys.* **87** 1117–57
[30] Yoshida H 1990 *Phys. Lett.* A **150** 262–8
[31] Suzuki M 1991 *J. Math. Phys.* **32** 400–7
[32] López-Lemus J and Alejandre J 2002 *Mol. Phys.* **100** 2983–92
[33] Panagiotopoulos A Z, Quirke N, Stapleton M and Tildesley D J 1988 *Mol. Phys.* **63** 527–45
[34] Mecke M, Winkelmann J and Fischer J 1997 *J. Chem. Phys.* **107** 9264–70
[35] Blokhuis E M, Bedeaux D, Holocomb C D and Zollweg J A 1995 *Mol. Phys.* **85** 665–9
[36] Liu Y and Tuckerman M E 2000 *J. Chem. Phys.* **112** 1685–700
[37] Allen M P and Schmid F 2006 *Preprint* cond-mat/0606511
[38] Sergi A, Ferrario M and Costa N 1999 *Mol. Phys.* **97** 825–32